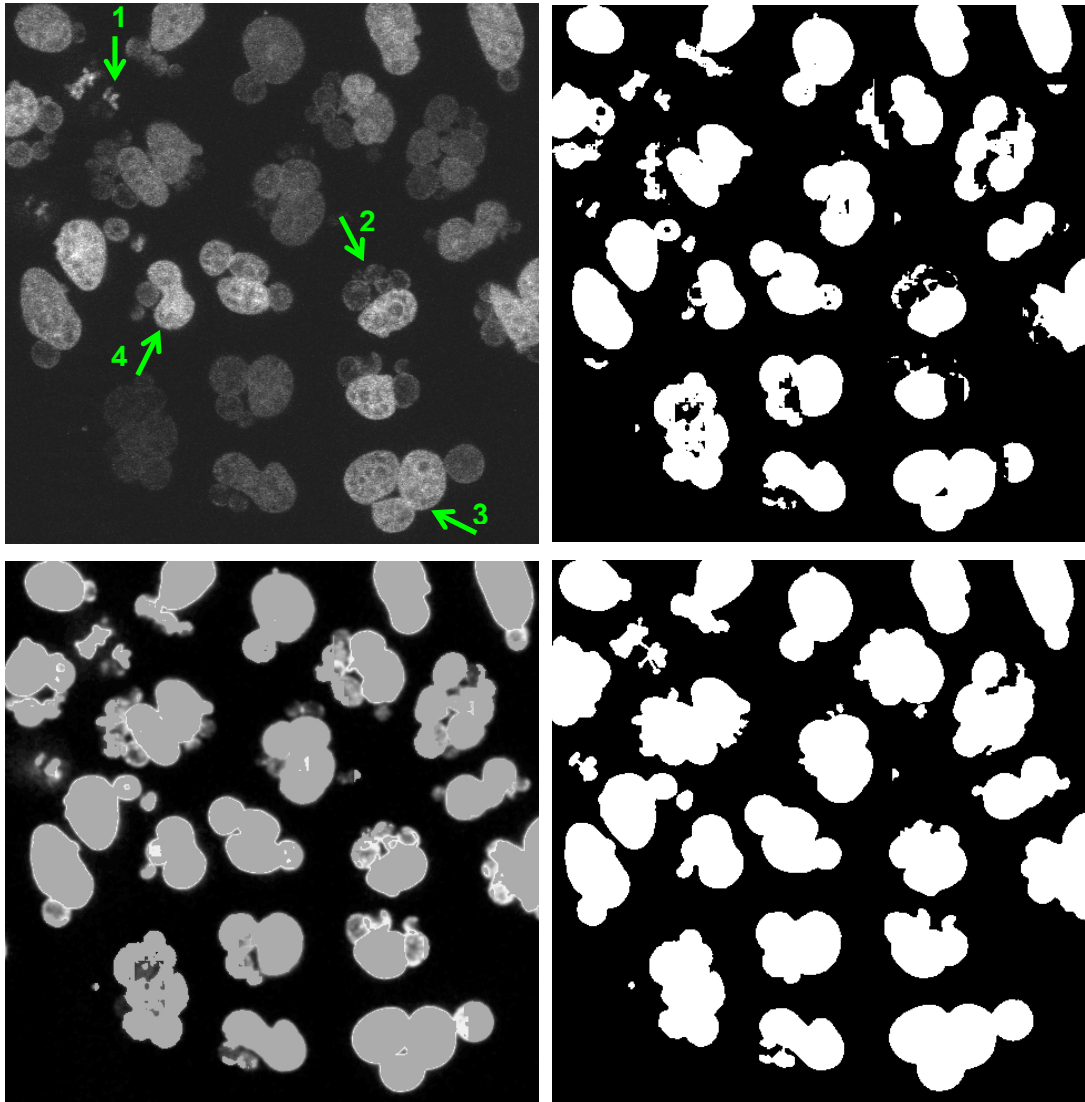
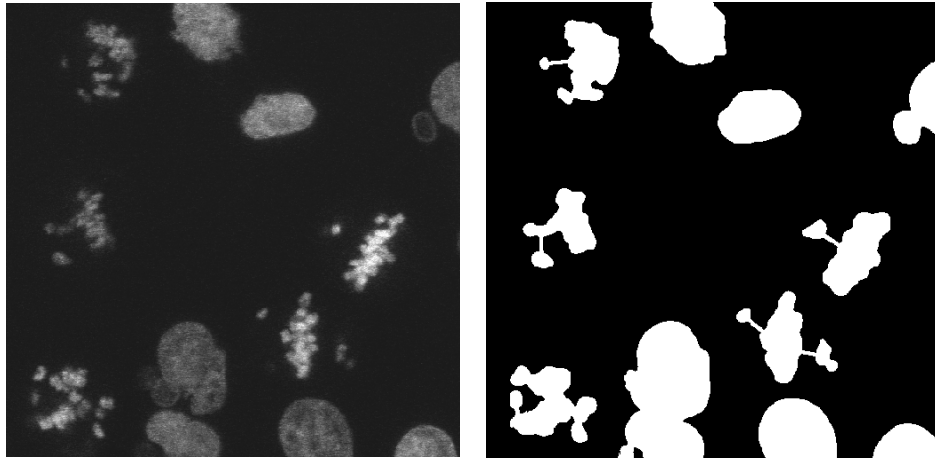


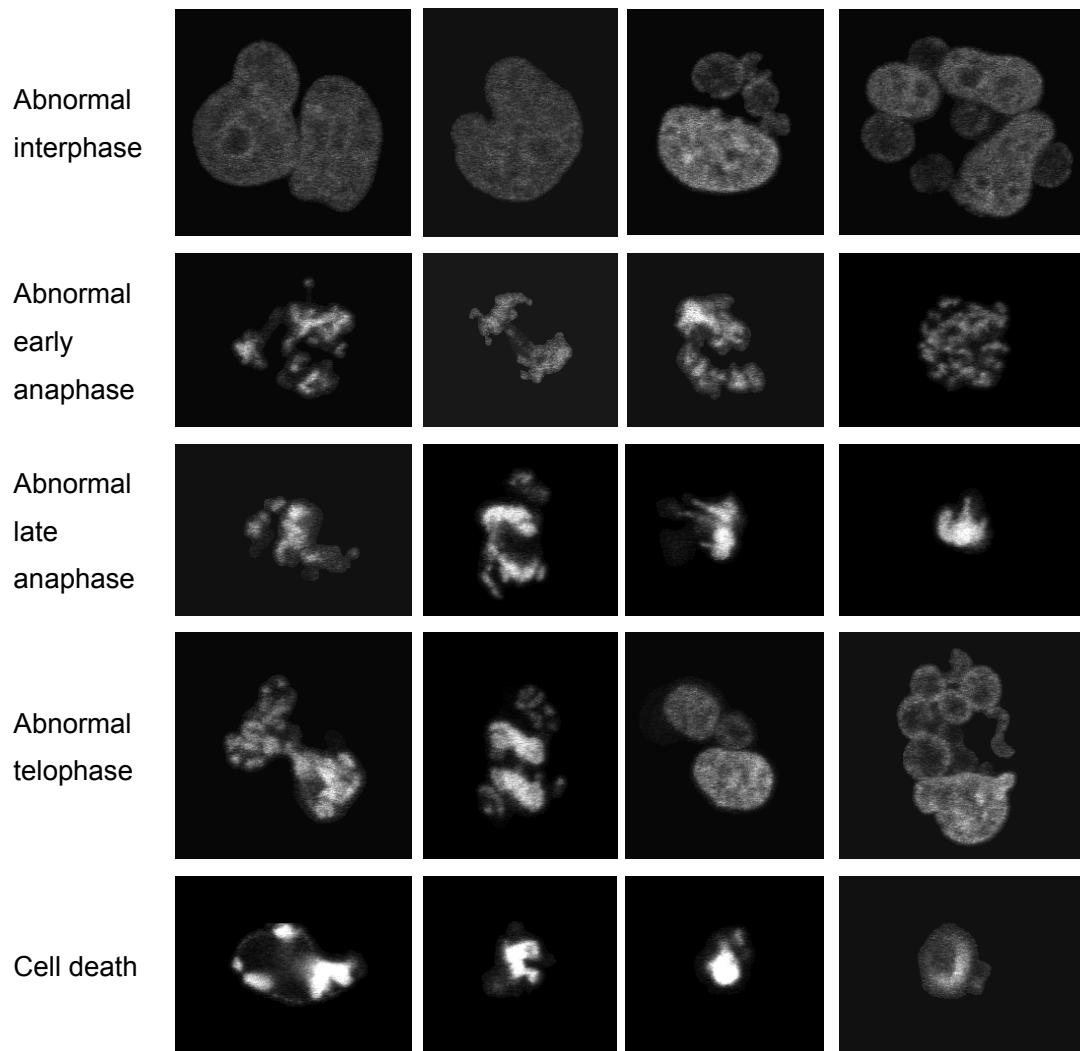
A



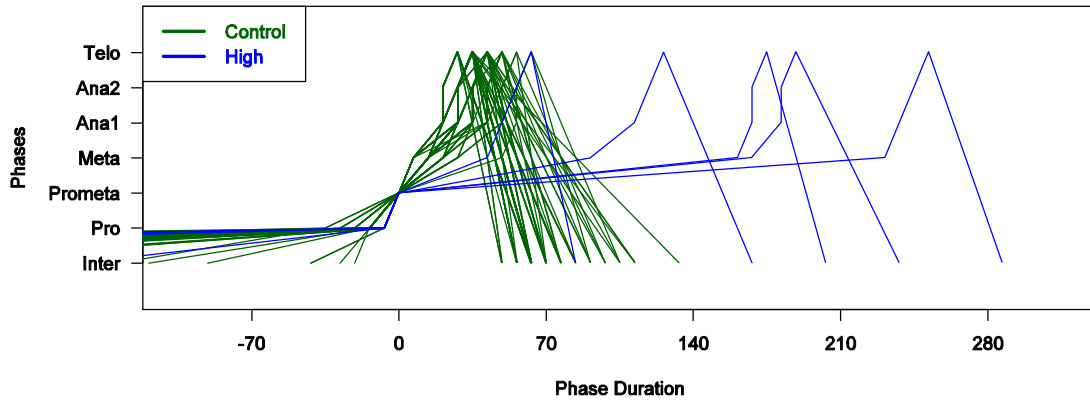
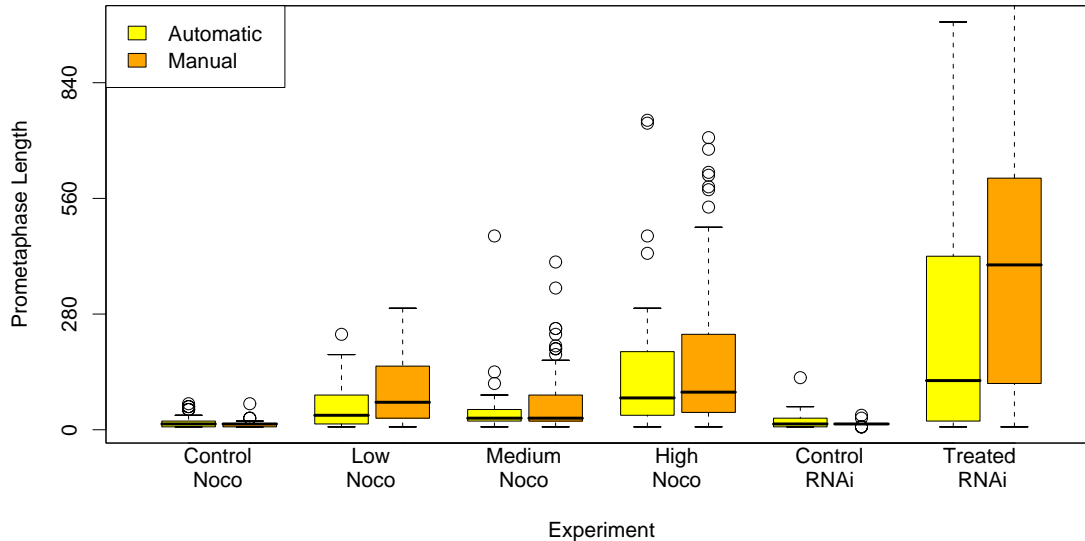
**B**



**Figure S1.** (A) Segmentation of images with diverse morphological phenotypes caused by microtubule perturbation (here caused by nocodazole or RNAi depletion which produces similar phenotypes): detached chromosomes (1), small and dark micronuclei (2), multinucleated cells (3), and non-spheroidal nuclei (4). (Top left) original image, (top right) initial segmentation: result after first run of region adaptive segmentation, (bottom left) original image overlaid with the initial segmentation as mask, (bottom right) result of region adaptive thresholding of the masked image. (B) Merging of detached chromosomes to corresponding prometaphase nuclei. Original image (left) and segmentation result (right).



**Figure S2.** Additional example images for the abnormal phenotype classes and class cell death taken from the training data set.

**A****B**

**Figure S3. (A)** Example phase sequences for single cells based on automated annotation of control and nocodazole treated cells. The phase sequences are temporally aligned at the transition between prophase and prometaphase. X-axis: phase length in minutes, **(B)** Boxplot of prometaphase length for all nocodazole concentrations and for the scr control and RNAi depletion of CKAP5, automated and manual annotation.

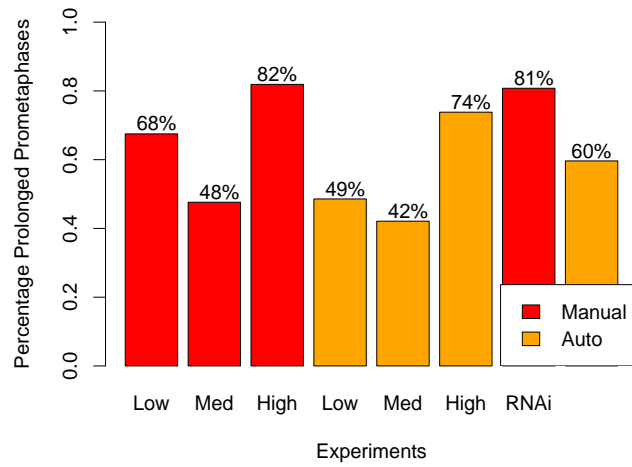


**Figure S4.** Percentage of prolonged prometaphases in the treated experiments, determined using the significance thresholds given in supplemental Table S6.

### Treated RNAi CKAP5



**Figure S5.** Sample image sequence with automatic annotation for one cell nucleus of the RNAi treated experiments.

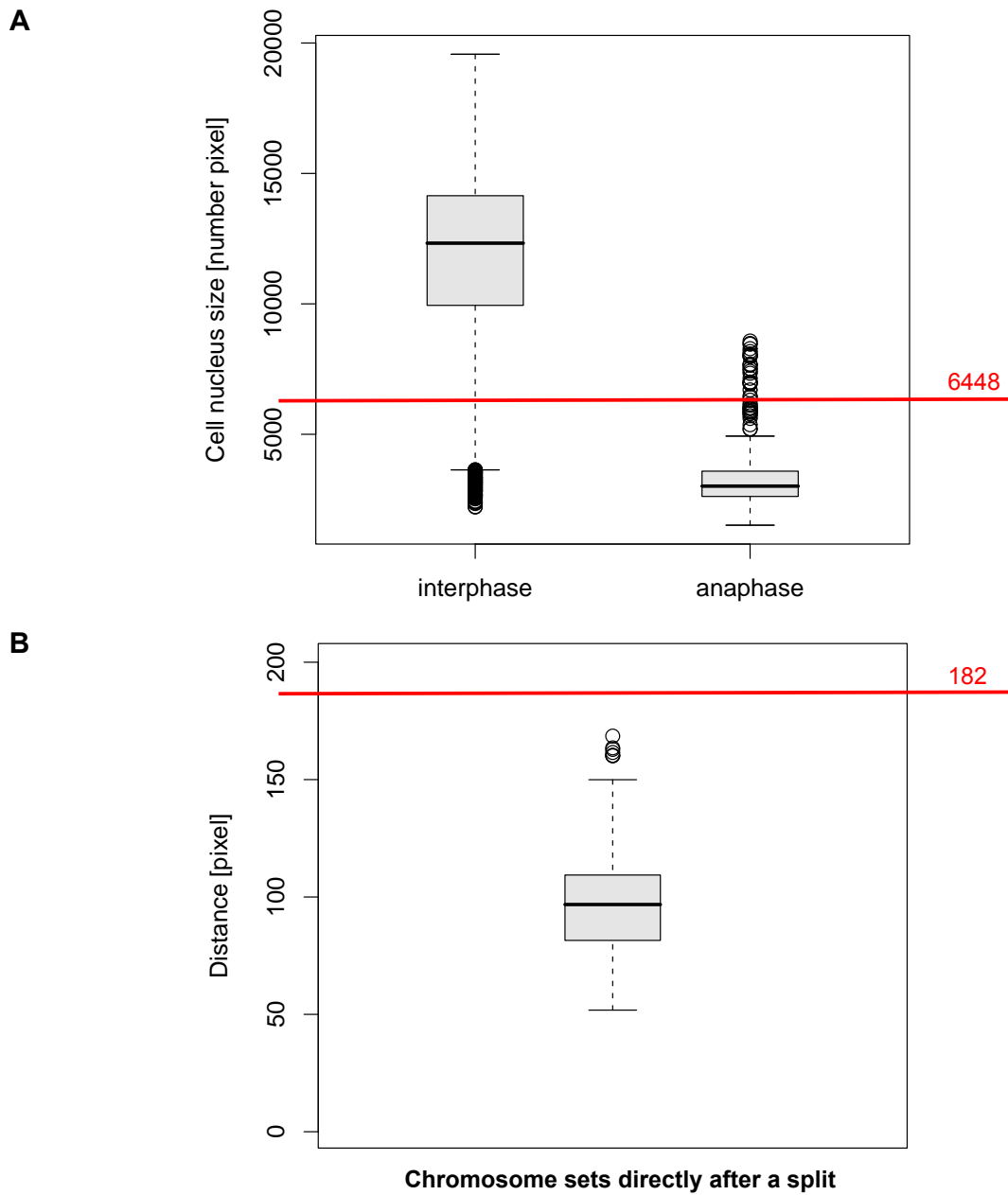


**Figure S6.** Verification of parameters for mitosis detection. **(A)** Boxplot of the cell nucleus sizes for all interphase and anaphase samples in the ground truth data set. The red line represents the threshold of 6448 defined by  $c_1 \cdot \text{mean cell size}$ , where  $c_1=0.6$  and the mean cell nucleus size over all contained cell nuclei was 10746. **(B)** Boxplot of the sibling distances (i.e. distances of daughter cells directly after splitting) based on the ground truth data set. The red line represents the threshold of 182 defined by  $c_2 \cdot \text{mean cell radius}$ . The upper edge of each box represents the 75%

quantile, the bold line within the box the median, and the lower edge of the box represents the 25% quantile. The whiskers reach at maximum 1.5 times the interquartile range, the circles are outliers above or below the range of the whiskers.

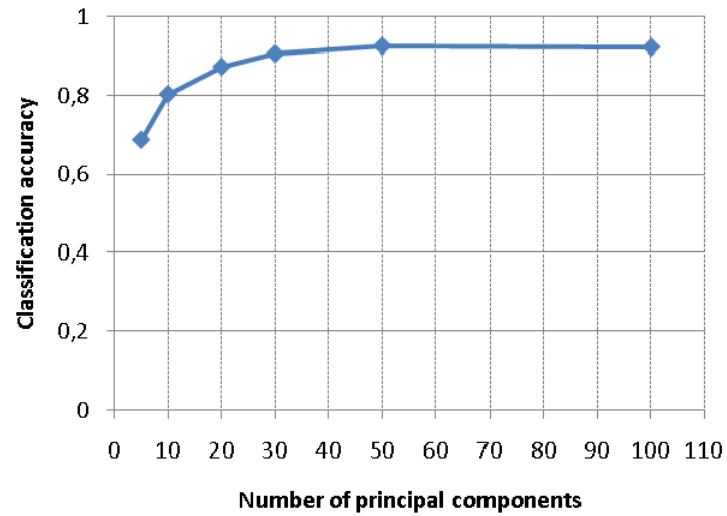


**Figure S7.** Classification accuracy for increasing numbers of principal components.

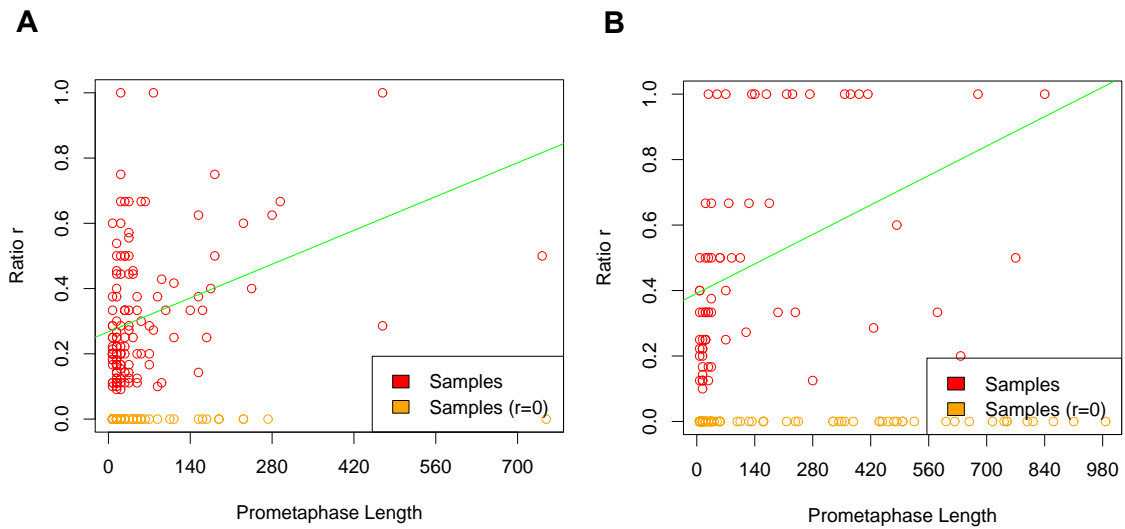


**Figure S8.** Correlation between prolonged prometaphase and ratio  $r$  for the automatically annotated nocodazole **(A)** and RNAi **(B)** data, respectively. After excluding samples with  $r = 0$  (orange points) a regression line (green) was fit to the data.  $R^2$  (fraction of variance explained by the model) for **(A)** and **(B)** is 0.13 and 0.17, respectively.

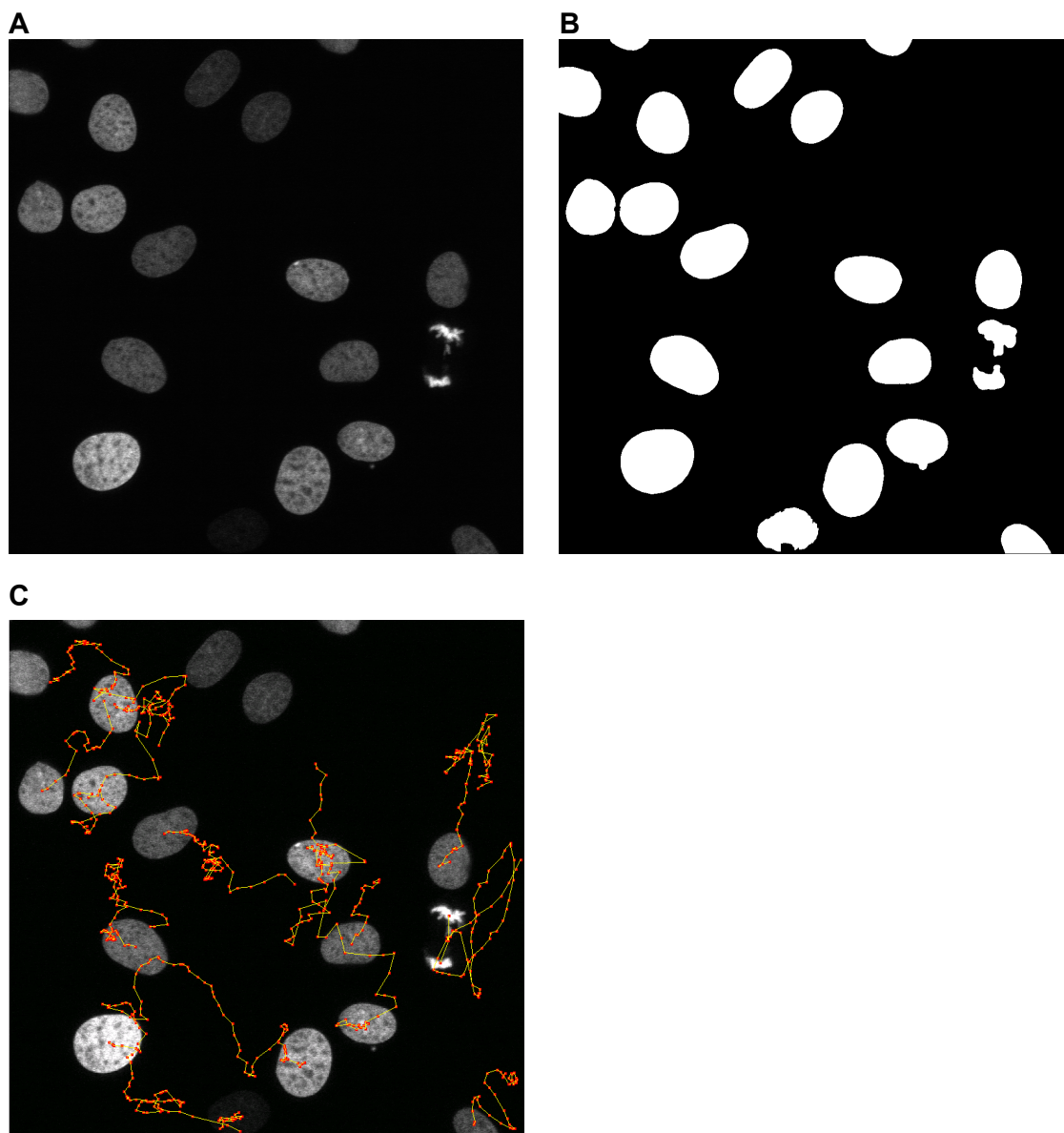


**Figure S9.** Example images for NRK (normal rat kidney) cells acquired on the LSM 510 Meta point scanning microscope. **(A)** Original image, **(B)** segmentation result, and **(C)** tracking result (red dots: centers-of-gravity, yellow lines: trajectories).

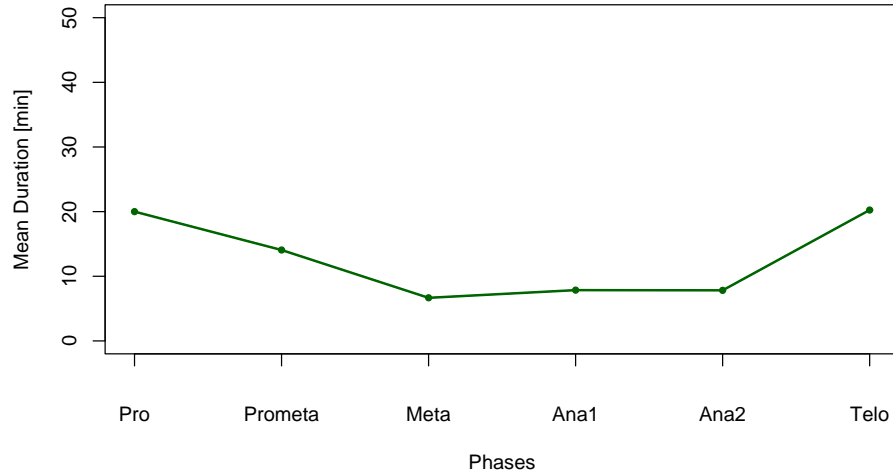


**Figure S10.** Automatically determined mean phase lengths for a different cell line (NRK, normal rat kidney cells). The analysis was based on six image sequences (acquired on the LSM 510 Meta point-scanning microscope).

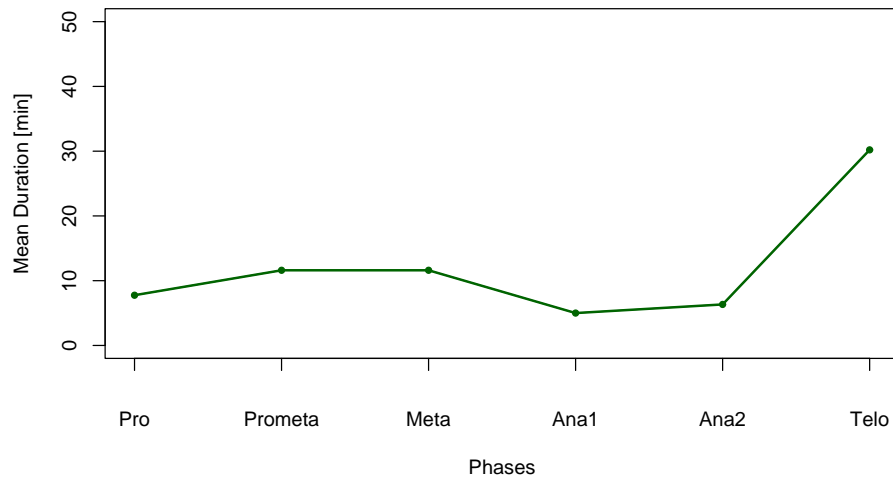


**Figure S11.** Automatically determined mean phase lengths for a different screening platform (LSM 5 LIVE line-scanning microscope). The analysis was based on four image sequences of HeLa cells.